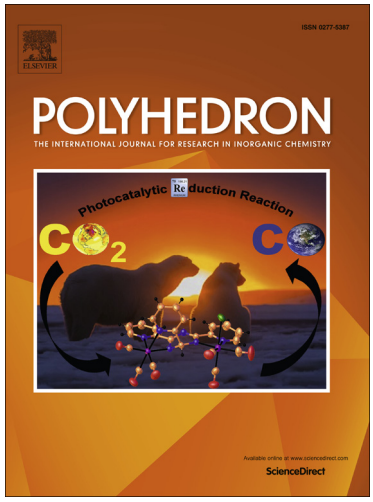

Dioxidomolybdenum(VI) complexes of tridentate ONO donor aroylhydrazones: Syntheses, spectral and structural characterization

A. Ambili Aravindakshan, Bibitha Joseph, U.L. Kala, M.R. Prathapachandra Kurup

PII: S0277-5387(16)30624-6
DOI: http://dx.doi.org/10.1016/j.poly.2016.11.033
Reference: POLY 12341

To appear in: *Polyhedron*

Received Date: 3 October 2016
Revised Date: 9 November 2016
Accepted Date: 13 November 2016

Please cite this article as: A. Ambili Aravindakshan, B. Joseph, U.L. Kala, M.R. Prathapachandra Kurup, Dioxidomolybdenum(VI) complexes of tridentate ONO donor aroylhydrazones: Syntheses, spectral and structural characterization, *Polyhedron* (2016), doi: http://dx.doi.org/10.1016/j.poly.2016.11.033

Dioxidomolybdenum(VI) complexes of tridentate ONO donor aroylhydrazones: Syntheses, spectral and structural characterization

A. Ambili Aravindakshan[a], Bibitha Joseph[a], U.L. Kala[b], M.R. Prathapachandra Kurup[a,*]

[a]*Department of Applied Chemistry, Cochin University of Science and Technology, Kochi 682 022, Kerala, India*

[b]*Department of Chemistry, Sree Narayana College, Nattika, Thrissur, Kerala, India*

Abstract

Four dioxidomolybdenum(VI) complexes, $[MoO_2(L^1)(H_2O)]$ (**1**), $[MoO_2(L^1)(H_2O)]\cdot(4,4'\text{-bipy})$ (**2**), $[(MoO_2(L^1))_2(4,4'\text{-bipy})]\cdot 2H_2O$ (**3**) and $[MoO_2(L^2)(DMF)]$ (**4**), of two tridentate ONO donor aroylhydrazones, H_2L^1 and H_2L^2 (where H_2L^1 = 3-methoxy-2-hydroxybenzaldehyde-2-furoic acid hydrazone and H_2L^2 = 4-benzyloxy-2-hydroxybenzaldehyde-4-nitrobenzoic hydrazone), have been synthesized and characterized by partial elemental analyses, molar conductivity measurements, FT-IR and electronic spectral studies. A distorted octahedral geometry was established for all the complexes using single crystal XRD studies. In all the complexes, the aroylhydrazone coordinates to the MoO_2^{2+} core through the phenolate oxygen, azomethine nitrogen and iminolate oxygen atoms, furnishing a vacant coordination site that can be utilized for binding of substrates like solvents or heterocyclic bases. The monomeric complexes $[MoO_2(L^1)(H_2O)]$ (**1**) and $[MoO_2(L^2)(DMF)]$ (**4**) were formed by the stoichiometric reaction of $MoO_2(acac)_2$ with the respective aroylhydrazones. The reaction of H_2L^1 with $MoO_2(acac)_2$ and 4,4′-bipyridine in an equimolar ratio yielded the 4,4′-bipyridine adduct $[MoO_2(L^1)(H_2O)]\cdot(4,4'\text{-bipy})$ (**2**), whereas the binuclear complex $[(MoO_2(L^1))_2(4,4'\text{-bipy})]\cdot 2H_2O$ (**3**) was formed, in which 4,4′-bipyridine acts as a conjugated bidentate

* *Corresponding author*
E mail address: mrpcusat@gmail.com, mrp_k@yahoo.com (M.R. Prathapachandra Kurup)
Phone: +91-484-2862423
Fax: +91-484-2575804

linker between two molybdenum centers, by taking twice the molar concentration of 4,4′-bipyridine.

Keywords: Aroylhydrazones; Dioxidomolybdenum(VI) complexes; Heterocyclic bases; IR spectra; Crystal structures

1. Introduction

Aroylhydrazones and their transition metal complexes have fascinated researchers on account of their potential implications in multifarious fields like medicine [1-3], catalysis [4], non-linear optics [5], magnetism etc [6]. Among the transition metals, molybdenum is a versatile biometal which has the ability to promote facile electron-transfer pathways, a consequence of the easy inter-convertibility of the different oxidation states, and permits facile ligand exchange reactions through the formation of stable and labile complexes with nitrogen, oxygen or/and sulfur donor atoms [7,8]. This intrinsic feature enables molybdenum to form complexes that function as efficient catalysts in oxotransferase reactions [9] as well as excellent models for molybdoenzymes [10]. Molybdenum complexes of the dibasic tridentate ligand system are especially significant and have been widely studied because they afford MoO_2L or MoOL complexes with accessible coordination sites that can be exploited for substrate binding [8,11,12]. Dioxidomolybdenum complexes have been reported to show remarkable catalytic activities in several organic transformation reactions which are employed in industrial processes such as epoxidation of olefins [13], oxidation of sulfides and olefins [14], oxidative cleavage of glycols [15] etc. Dioxidomolybdenum complexes have also been investigated for their biological relevance [16-19] and they occupy a significant place within the scope of the fundamental chemistry of this metal.

The design and development of synthetic methodologies for compounds with diverse structures and supramolecular architectures are quite interesting as well as challenging too. Coordination frameworks extending from mononuclear to multinuclear centres can be assembled by controlling reaction parameters like the inherent coordination geometry of the metal ion, nature and bonding versatility of the ligands used, metal-ligand ratio, pH values of the reaction medium and solvents employed [20,21]. The syntheses of binuclear complexes derived from a dibasic ligand system can

be achieved by employing neutral linear N,N′-bidentate spacers like 4,4′-bipyridine (4,4′-bipy), *trans*-1,2 bis(4-pyridyl)ethane, *trans*-1,2 bis(4-pyridyl)ethane, 4,4′-bipyridine-N,N′-dioxide etc. as bridging ligands [22,23]. These extended polypyridyl type bridging ligands are found to be excellent and have the ability to connect two coordinatively unsaturated metal centers, which in turn produce mixed-valence complexes as well as molecular wires [24]. The supramolecular frameworks in the crystal lattices are stabilized through various intermolecular and non-covalent forces like hydrogen bonds, $\pi\cdots\pi$ and C–H$\cdots\pi$ interactions [25].

In this paper, we report the syntheses as well as structural characterization of four dioxidomolybdenum(VI) complexes of the aroylhydrazones H_2L^1 and H_2L^2 (where H_2L^1 = 3-methoxy-2-hydroxybenzaldehyde-2-furoic acid hydrazone and H_2L^2 = 4-benzyloxy-2-hydroxybenzaldehyde-4-nitrobenzoic hydrazone), in which three of them are mononuclear and the remaining one is binuclear in nature. The supramolecular interactions present in structures of the complexes, arising from different solvents (DMF and H_2O) as well as the heterocyclic bidentate linker 4,4′-bipy which was added to complete the sixth labile coordination site of the dioxidomolybdenum(VI) complexes, have been also discussed.

2. Experimental section

2.1. Materials

3-Methoxy-2-hydroxybenzaldehyde (Alfa Aesar), 4-benzyloxy-2-hydroxybenzaldehyde (Sigma-Aldrich), 2-furoic acid hydrazide (Sigma-Aldrich), 4-nitrobenzoic hydrazide (Sigma-Aldrich), $MoO_2(acac)_2$ (Sigma-Aldrich) and the heterocyclic base, like 4,4′-bipyridine (Sigma-Aldrich), were of Analar grade and purchased from commercial sources. The solvents methanol (Spectrochem) and DMF (Spectrochem) were used without further purification. The ligand H_2L^1 was obtained by the condensation of equimolar mixtures of methanolic solutions of 3-methoxy-2-hydroxybenzaldehyde and 2-furoic acid hydrazide and the product was formed *in situ*. The ligand H_2L^2 was prepared and isolated as $H_2L^2\cdot C_3H_7NO$ by an earlier reported method [26]. The structural formulae of the aroylhydrazones H_2L^1 and H_2L^2 are represented in Scheme 1.

Scheme 1

2.2.1. Syntheses of the dioxidomolybdenum(VI) complexes

*2.2.2.1. Synthesis of [$MoO_2(L^1)(H_2O)$] (**1**)*

Methanolic solutions of 3-methoxy-2-hydroxybenzaldehyde (0.1521 g, 1 mmol) and 2-furoic acid hydrazide (0.1261 g, 1 mmol) were mixed and refluxed in a water bath for six hours. To this solution, $MoO_2(acac)_2$ (0.3262 g, 1 mmol) dissolved in hot methanol and 4 drops of con. HCl were added and the resulting orange colored solution was refluxed for six hours. The solution was then kept for evaporation at room temperature and an orange precipitate formed. Single crystals of the compound were isolated by recrystallization from a DMF-methanol mixture within four weeks. The product obtained was filtered and dried. Yield: 0.2222 g (55%).

*2.2.2.2. Synthesis of [$MoO_2(L^1)(H_2O)$]·(4,4'-bipy) (**2**)*

Methanolic solutions of 3-methoxy-2-hydroxybenzaldehyde (0.1521 g, 1 mmol) and 2-furoic acid hydrazide (0.1261 g, 1 mmol) were mixed and refluxed in a water bath for six hours. To this solution, 4,4′-bipyridine (0.1561 g, 1 mmol) and $MoO_2(acac)_2$ (0.3262 g, 1 mmol) dissolved in hot methanol were added and the resulting orange colored solution was refluxed for 6 hours. An orange colored precipitate separated out and single crystals of the compound were isolated by recrystallization from a DMF-methanol mixture within three weeks. The product obtained was filtered and dried. Yield: 0.4090 g (73%)

*2.2.2.3. Synthesis of [$(MoO_2(L^1))_2$(4,4'-bipy)]·$2H_2O$ (**3**)*

Methanolic solutions of 3-methoxy-2-hydroxybenzaldehyde (0.1521 g, 1 mmol) and 2-furoic acid hydrazide (0.1261 g, 1 mmol) were mixed and refluxed in a water bath for six hours. To this solution, 4,4′-bipyridine (0.3123 g, 2 mmol) and $MoO_2(acac)_2$ (0.3262 g, 1 mmol) dissolved in hot methanol were added and the resulting orange colored solution was refluxed for 6 hours. An orange colored precipitate separated out and single crystals of the compound were isolated by recrystallization from a DMF-methanol mixture within four weeks. The product obtained was filtered and dried. Yield: 0.6814 g (72%).

*2.2.2.4. Synthesis of [$MoO_2(L^2)(DMF)$] (**4**)*

To a solution of aroylhydrazone, H_2L^2 (0.4640 g, 1 mmol) in DMF, $MoO_2(acac)_2$ (0.3260 g, 1 mmol) in DMF was added. The resultant solution was refluxed for 4 hours. This was cooled and the orange colored crystalline complex that formed was collected, washed with methanol, followed by ether and dried over P_4O_{10} *in vacuo*. Single crystals of [$MoO_2(L^2)(DMF)$] (**4**) were obtained by recrystallization of the compound from DMF. Yield: 0.3956 g (67%).

2.3. Physical measurements

Carbon, hydrogen and nitrogen analyses were carried out using a Vario EL III CHNS analyzer. Infrared spectra were recorded on a JASCO FT-IR-5300 spectrometer in the range 4000-400 cm^{-1} using KBr pellets. Electronic spectra were recorded on a Thermo Scientific Evolution 220 model UV-Visible spectrophotometer in the 50000-10000 cm^{-1} range using solutions in DMF. Molar conductivities of the complexes in DMF solutions (10^{-3} M) at room temperature were measured using a Systronic model 303 direct reading conductivity meter.

2.4. X-ray crystallography

Single crystal of complexes **1**-**4** with suitable dimensions were selected and mounted on a Bruker SMART APEXII CCD diffractometer, equipped with a graphite crystal, incident-beam monochromator and a fine focus sealed tube with Mo Kα (λ = 0.71073 Å) radiation as the X-ray source. The unit cell dimensions were measured and the data collection was performed at 292(2) K. The programs SAINT and XPREP were used for data reduction and APEX2 and SAINT were used for cell refinement [27]. Absorption corrections were carried out using SADABS based on Laue symmetry using equivalent reflections [28]. The structures were solved by direct methods and refined by full-matrix least-squares refinement on F^2 using SHELXL-97 and SHELXL-2014/7 [29] provided in WinGX [30]. The molecular and crystal structures were plotted using DIAMOND version 3.2g [31].

In all the complexes, anisotropic refinements were performed for all non-hydrogen atoms and all H atoms on C atoms were placed in calculated positions, guided by difference maps, with C–H bond distances of 0.93-0.96 Å. H atoms were assigned as U_{iso} = 1.2U_{eq} (1.5 for Me). The hydrogen atoms (H7A and H7B in **1** / H1 and H1' in **2** / H1D and H1E in **3**) attached to the oxygen atom of the coordinated water molecule in **1** and **2** as well as the lattice water molecule in **3** were located from difference maps and their distances and angles were restrained using DFIX and DANG instructions with distance restraints of O–H = 0.86±0.01 and H···H = 1.36±0.02 Å, followed by refinement of their displacement parameters. The reflections (1 0 0), (-2 8 3) and (0 1 1) in **1**, (0 0 1), (0 1 1), (1 1 0) and (1 0 1) in **2**, (0 1 1), (0 0 1), (0 1 0) and (-1 1 4) in **3** and (0 0 1), (-1 1 1), (-1 0 1) and (0 1 0) in **4** were omitted owing to bad disagreement. In $[MoO_2(L^1)(H_2O)]\cdot$(4,4′-bipy) (**2**), the extinction coefficient has a value of 0.0127(11). The crystallographic data and structure refinement parameters for compounds **1**-**4** are given in Table 1.

Table 1

3. Results and discussion

Four dioxidomolybdenum(VI) complexes of two different tridentate ONO aroylhydrazones were synthesized and characterized. Complexes **1** and **4** were afforded by the stoichiometric reaction of $MoO_2(acac)_2$ with the aroylhydrazones in DMF-methanol or DMF reaction media. The reaction of an aroylhydrazone, $MoO_2(acac)_2$ and 4,4′-bipyridine in equimolar ratios yielded the 4,4′-bipyridine adduct of dioxidomolybdenum(VI), complex **2**, whereas when the ratio of the reactants was changed from 1:1:1 to 1:1:2, the binuclear complex **3** was formed in which 4,4′-bipyridine acts as linker between two molybdenum centers. The complexes were characterized by various physico-chemical methods, such as partial elemental analyses, molar conductivity measurements, FT-IR and electronic spectral analyses. We were also successful in isolating single crystals of compounds **1**-**4** and their structures were established by single crystal X-ray diffraction studies.

All the dioxidomolybdenum(VI) complexes are soluble in solvents like DMF and DMSO, partially soluble in acetonitrile and insoluble in solvents like methanol and ethanol.

The analytical data of the complexes are given in Table 2. The partial elemental analyses of the complexes suggest that all the complexes are analytically pure and correspond to mononuclear complex motifs with the general formula $[MoO_2(L)(X)]$, where L is the bideprotonated aroylhydrazone and X is the solvent (H_2O or DMF), for all the complexes except **3** in which two $[MoO_2(L)]$ moieties are connected by a conjugated bidentate 4,4′-bipyridine linker, resulting in a dimeric complex. In all the complexes, the aroylhydrazone ligand is coordinated in the bideprotonated iminolate form, which is evident from the IR spectral analyses. The molar conductivity measurements of all the compounds in DMF (10^{-3} M) at room temperature suggests that all the complexes are non-electrolytic in nature and remain undissociated in DMF [32].

Table 2

3.1. IR spectra

The tentative assignments for the significant IR spectral bands of the dioxidomolybdenum(VI) complexes are presented in the Table S1. The aroylhydrazones H_2L^1 and H_2L^2 displayed distinct bands in the regions 1597-1609, 1680-1580, 3067-3186, 3377-3505 and 1102-1127 cm^{-1}, corresponding to the ν(C=N), ν(C=O), ν(N–H), ν(O–H) and ν(N–N) stretching vibrations, which are indicative of the existence of the amido form of the ligand in the solid state [33,34]. The bands due to ν(C=O) and ν(N–H) are absent in the complexes, suggesting the occurrence of amido-iminol tautomerization following the deprotonation of the ligands during complexation [34a,34d]. The shift of the ν(C=N) absorption towards lower frequency in all the complexes indicates the coordination of the azomethine nitrogen atom to the metal center [34a,34d]. The disappearance of the intense bands attributed to –C=O stretching vibrations along with appearance of new bands in the 1543-1630 cm^{-1} region due to the asymmetric stretching vibration of the newly formed C=N bond justifies the iminolization of the aroylhydrazone ligand in these complexes [35]. The presence of lattice water in complex **3** was confirmed from the broad band obtained above 3400 cm^{-1} [36,37].

All the dioxidomolybdenum(VI) complexes exhibit two bands in the 890-915 and 920-970 cm^{-1} regions and can be assigned to symmetric and asymmetric vibrations respectively, characteristic of *cis*-MoO_2 cores as reported in the literature [12,38]. The

weak band in the 550-610 cm^{-1}region in the metal complexes has been assigned to the ν(Mo–N) vibration mode [18,39]. The medium intensity bands at 814, 1217 and 1405 cm^{-1} in **2** and 1226 and 1407 cm^{-1} in **3** corresponds to the stretching vibrations of the free as well as coordinated bidentate 4,4′-bipyridine ligand respectively [40].

3.2. Electronic spectra

The electronic spectral assignments of the dioxidomolybdenum(VI) complexes in DMF solution are summarized in Table S2. The electronic spectra of the aroylhydrazones show bands in the 32600-38200 cm^{-1} region due to n→π*/π→π* transitions [8,34b,34c]. These bands suffer a considerable shift in intensity and wavelength on coordination [8,34a,34d]. The complexes show broad bands in the 21110-29000 cm^{-1} region which may be assigned to ligand to metal charge transfer transitions [8].

3.3. Description of the crystal structures

*3.3.1. General features in the molecular structures of $[MoO_2(L^1)(H_2O)]$ (**1**), $[MoO_2(L^1)(H_2O)]\cdot(4,4'\text{-bipy})$ (**2**), $[(MoO_2(L^1))_2(4,4'\text{-bipy})]\cdot 2H_2O$ (**3**) and $[(MoO_2(L^2)(DMF)]$ (**4**)*

The coordination geometry around the molybdenum(VI) atom shows a distorted octahedral environment with an NO_5 (for **1**, **2** and **4**) or N_2O_4 (for **3**) chromophore. The coordination geometry was satisfied by the bideprotonated tridentate ONO donor aroylhydrazone ligand, through the phenolate oxygen, azomethine nitrogen and iminolate oxygen atoms, and terminal oxo groups. The sixth labile site is occupied by an oxygen atom of solvent water in **1** and **2**, a nitrogen atom of the heterocyclic bidentate linker in **3** and an oxygen atom of solvent DMF in **4**. The equatorial positions of the octahedron are defined by the donor atoms of the aroylhydrazone ligand and one of the terminal oxo oxygen atoms, whereas the axial positions are occupied by another terminal oxo oxygen atom and the oxygen atom of the solvent water/nitrogen atom of the heterocyclic base. In all the complexes, the aroylhydrazone ligand is coordinated to the *cis*-MoO_2^{2+} core in a meridional fashion, forming five and six membered metallocycles involving the MoO_2^{2+} center. The large as well as weak Mo–X distances (X = oxygen atom of the solvent

molecule in **1**, **2** and **4** or the nitrogen atom of the heterocyclic base in **3**), in comparison with the other Mo–N, Mo–O bond distances in the complex, substantiate the respective position to hold the possibility of functioning as a substrate binding site. In all cases the Mo atom is displaced by 0.3-0.5 Å from the square plane towards the terminal oxo oxygen atom at a distance of 1.9-2.1 Å from this plane, leading to the shrinking of the bond length of the *trans* oxo oxygen atom as well as lengthening the Mo–X bond. The Mo–O, Mo–N and Mo=O bonds are within their normal ranges and are comparable to those observed in other similar dioxidomolybdenum(VI) complexes [19,22,23,35]. The aroylhydrazone ligand is coordinated in the iminolate form in the complexes, which is evidenced by the bond distances C9–O3 (1.30-1.33 Å) and N2–C9 (1.29-1.32 Å) [8]. The bond lengths C=N_{azo} and N_{azo}–N_{imine} also show the extensive delocalization in the coordinated hydrazine ligand. The *cis*-MoO_2^{2+} unit forms five and six membered chelate rings with bite angles in the range 70-82° ($O_{phenolate}$–Mo–N_{azo} and $O_{iminolate}$–Mo–N_{azo}). The bond distances about the Mo center reveal the magnitude of the distortions, as can be seen in Table 3. The angular distortion in the octahedral environment around the Mo atom comes from the five and six membered chelate rings with the hydrazone ligand, so that the *trans* angles and *cis* angles significantly deviate from the ideal values of 180 and 90° respectively.

*3.3.1.1. Crystal structure of [$MoO_2(L^1)(H_2O)$] (**1**)*

The molecular structure of complex **1** along with the atom numbering scheme is shown in Fig. 1 and significant bond distances and bond angles are shown in Table 3. The complex crystallizes into the monoclinic space group, $P2_1/c$ with four molecules in the unit cell.

Fig. 1

Ring puckering analysis and least square plane calculations [41] show that in complex **1** the ring Cg(1), comprising of the atoms Mo(1), O(3), C(9), N(1) and N(2), is puckered with puckering amplitude Q(2) = 0.0788(19) Å and ϕ(2) = 15.4(18)º. The puckering of the five membered metallocycle was also calculated in terms of the pseudorotation parameter P and τ_m [42], and it was found that the metallocycle adopts twisted conformation with P = 190.7(13)º and τ = 7.7(1)º for reference bond Mo(1)–O(3)

in Cg(1). The metallocycle Cg(3), comprising of atoms Mo(1), O(2), C(7), C(6), C(8) and N(1), is also found to be puckered in complex **1** with puckering amplitude Q = 0.266(2) Å, θ = 117.4(4)° and ϕ = 223.6(6)°.

*3.3.1.2. Crystal structure of [$MoO_2(L^1)(H_2O)$]·(4,4′-bipy) (**2**)*

Orange block shaped single crystals of [$MoO_2(L^1)(H_2O)$]·(4,4′-bipy) (**2**) were isolated by slow evaporation of its mother liquor. The asymmetric unit of the compound consists of a [$MoO_2(L^1)(H_2O)$]·molecule and half of a 4,4′-bipyridine molecule. There is an inversion center at the midpoint of the C14···C14A bond of the 4,4′-bipyridine molecule. The complex is crystallized as the 4,4′-bipyridine adduct in the triclinic space group, $P\bar{1}$. The bond lengths and bond angles are comparable to similar dioxidomolybdenum(VI) complexes in which 4,4′-bipyridine is present in the crystal lattice [11,43]. The molecular structure of complex **2** along with the atom numbering scheme is shown in Fig. 2.

Fig. 2

The ring puckering analysis and least square plane calculations [41] of complex **2** show that the six membered metallocycle Cg(3), comprising of atoms Mo(1), O(2), C(7), C(6), C(8) and N(1), is puckered with puckering amplitude Q = 0.300 Å, θ = 117.7(4)° and ϕ = 207.8(6)°. Conformational analyses [44] show that this six membered metallocycle Cg(3) adopts the S-form (screw-boat) conformation.

3.3.1.3. Crystal structure of [$(MoO_2(L^1))_2$(4,4′-bipy)]·2H_2O (3)

Reddish orange block shaped single crystals of [$(MoO_2(L^1))_2$(4,4′-bipy)]·2H_2O (**3**) were isolated by slow evaporation of its mother liquor. This complex crystallizes in the triclinic space group, $P\bar{1}$, possessing a crystallographic center of inversion. The molecular structure of complex **3**, along with the atom numbering scheme, is shown in Fig. 3 and the description of the structure is limited to half of the molecule.

Fig. 3

Two [MoO_2(L)] units in complex **3** are bridged together through the nitrogen atoms of the 4,4′-bipyridyl ligand to form a dinuclear dioxidomolybdenum(VI) complex with a Mo···Mo separation of 11.9865(5) Å; this is comparable to similar binuclear

dioxidomolybdenum(VI) complexes in which the metal centers are connected by a 4,4′-bipyridine linker [19,22,23,45]. Ring puckering analysis and least square plane calculations [41] show that the ring Cg(3) in complex **3**, comprising of atoms Mo(1), O(2), N(1), C(6), C(7) and C(8), is puckered with puckering amplitude Q = 0.3500(18) Å, θ = 119.2(3)° and ϕ = 189.2(5)º.

*3.3.1.4. Crystal structure of [$MoO_2(L^2)$(DMF)] (**4**)*

The molecular structure of the complex **4**, with the atom numbering scheme, is shown in Fig. 4 and relevant bond distances and angles are presented in Table 3. The complex crystallizes in the triclinic space group $P\bar{1}$. There are two crystallographically independent molecules in the asymmetric unit of the compound (Fig. 4) with bond lengths and angles which agree with each other.

Fig. 4

Ring puckering analysis and least square plane calculations [41] show that the rings Cg(2) and Cg(7) in complex **4**, involving the Mo(1) and Mo(2) centers, are found to be puckered. The six membered metallocycle Cg(2), comprising of the atoms Mo(1), O(2), C(10), C(11), C(14) and N(1), is puckered with puckering amplitude Q = 0.250(2) Å, θ = 60.3(7)° and ϕ = 21.4(8)º. Similarly, the six membered metallocycle Cg(7), comprising of the atoms Mo(2), O(10), C(34), C(35), C(38) and N(5), is also puckered with puckering amplitude Q = 0.294(2) Å, θ = 116.4(6)° and ϕ = 190.2(7)º.

*3.3.2. Supramolecular features in complexes **1**-**4***

The interaction parameters for complexes **1**-**4** are listed in Table S3. In [$MoO_2(L^1)(H_2O)$] (**1**), the oxygen atom of the coordinated water molecule acts as a hydrogen bond donor and is involved in intermolecular hydrogen bonds, namely O(7)–H(7A)···O(1), O(7)–H(7B)···O(4) and O(7)–H(7B)···N(2). These hydrogen bonds connect the molecules to form a supramolecular chain which propagates in the *b* direction when viewed along the crystallographic *a* axis (Fig. 5). The hydrogen atom H7B attached to O7 is involved in bifurcating hydrogen bonds with two acceptors, N2 and O4.

Fig. 5

Non-conventional hydrogen bonding interactions, like C(1)–H(1B)···O(5), C(12)–H(12)···O(3) and C(13)–H(13)···O(6), are also present in the crystal lattice of **1**. The hydrogen bonds, C(1)–H(1B)···O(5) and C(12)–H(12)···O(3) link adjacent molecules (Fig. S1). The hydrogen bond C(13)–H(13)···O(6), observed at a H···A distance of 2.33 Å and <(DHA) = 150.5°, connects the molecules in a linear fashion propagating along the *b* direction (Fig. 6).

Fig. 6

The crystal lattice packing in complex **1** is also further supported by π···π as well as O–H···π bonding interactions (Table S4). The six membered aromatic ring Cg(4) (comprising of atoms C2, C3, C4, C5, C6 and C7) of one aroylhydrazone moiety interacts with the five membered furan ring Cg(2) (comprising of atoms O4, C10, C11, C12 and C13) of another aroylhydrazone moiety through a π···π interaction with a distance of 3.6756 Å (Fig. S2). The hydrogen atom H7A attached to the O7 atom of the coordinated water molecule is involved in a O–H···Cg(1) interaction, in which Cg(1) is a five membered metallocycle comprising of atoms Mo1, O2, C9, N3 and N2. The unit cell crystal lattice packing is viewed along the *b* direction (Fig. S3).

The crystal packing of $[MoO_2(L^1)(H_2O)]\cdot$(4,4′-bipy) (**2**) is enriched with strong classical intermolecular hydrogen bonds (Fig. 7), in which the oxygen (O1W) atom of the coordinated water molecule acts as a donor for two different acceptors, N2 (imine nitrogen atom) and N3 (nitrogen atom of 4,4′-bipyridine). The hydrogen bond O(1W)–H(1)···N(2) connects adjacent molecules into dimers. One of the complex motifs in these dimers is connected to the nitrogen atom of a nearby 4,4′-bipyridine molecule through an O(1W)–H(1′)···N(3) hydrogen bond. There is a weak non-conventional C–H···O hydrogen bonding interaction involving the hydrogen atom H18 attached to the C18 atom of the 4,4′-bipyridine molecule and the oxo oxygen atom O6.

Fig. 7

The crystal lattice packing in complex **2** is also further supported by π···π as well as O–H···π interactions (Table S4) which is the same as observed in the case of complex **1**. The Cg(4) (comprising of atoms C2, C3, C4, C5, C6 and C7) and Cg(2) (comprising of atoms O4, C10, C11, C12 and C13) rings of adjacent aroylhydrazone moieties interact

with a distance of 3.873(2) Å. The O1W–H1···Cg(1) interaction is observed at a H···Cg distance of 2.66(3) Å, in which Cg(1) is a five membered metallocycle comprising of the atoms Mo1, O2, C9, N3 and N2. The unit cell crystal packing of **2** as viewed along the crystallographic *a* axis is given in Fig. S4.

The unit cell packing of $[(MoO_2(L^1))_2(4,4'\text{-bipy})]\cdot 2H_2O$ (**3**), featuring sliding H shaped complex motifs when viewed along the crystallographic *a* axis, is shown in Fig. 8. The crystal packing of complex **3** is strengthened by classical and non-classical inter- or intramolecular hydrogen bonds present in the lattice. The intramolecular hydrogen bonds C(14)–H(14)···O(6), C(18)–H(18)···N(1) and O(1S)–H(1E)···O(5) impart rigidity to the complex motif (Fig. S5).

Fig. 8

In complex **3**, the oxygen atom of the lattice water molecule, O1S, participates in bifurcating hydrogen bonds with two acceptors, atoms N2 and O4, through the hydrogen atom H1D. The non-conventional intermolecular hydrogen bonds C(8)–H(8)···O(5), O(15)–H(15)···O(1) and O(18)–H(18)···O(1S) assemble the complex motifs and form a one dimensional layer type chain in the crystal packing which propagates along the *bc* plane when viewed along the crystallographic *a* axis (Fig. 9). The *trans* oxo oxygen atom O5 serves as an acceptor for both conventional intramolecular (O(1S)–H(1E)···O(5)) as well as non-conventional intramolecular (C(8)–H(8)···O(5)) hydrogen bonding interactions. Similarly, the carbon atom attached to the 4,4′-bipyridine molecule is involved in the bifurcating hydrogen bonds with two acceptors, atoms N1 and O1S, for the formation of non-conventional intra as well as intermolecular hydrogen bonding interactions.

Fig. 9

In complex **3**, two π···π (between Cg(1)···Cg(4) and Cg(2)···Cg(2)) and two C(1)–H(1A)···Cg(5) and C(12)–H(12)···Cg(4) bonding interactions (Table S4) are observed in the crystal structure. There exists a weak π···π interaction between Cg(4) (comprised of atoms N3, C14, C15, C16, C17 and C18) interacting with Cg(1)

(comprised of atoms Mo1, O1, C9, N2 and N1) at a distance of 3.9660(13) Å. Another π···π interaction is observed between the furan rings (Cg(2)···Cg(2)) of adjacent molecules (Fig. S6). Weak C(1)–H(1A)···Cg(5) and C(12)–H(12)···Cg(4) bonding interactions are observed in the crystal packing (Fig. S7).

In $[MoO_2(L^2)(DMF)]$ (**4**), there are no conventional hydrogen bonds present in the molecular system. However, some weak interactions like π···π, C–H···π and C–H···O (Table S4) are observed in the crystal structure. The adjacent molecules are linked into chains by non-conventional hydrogen bonding interactions, as shown in Fig. 10. Rings Cg(9) and Cg(10) of neighboring molecules are involved in π···π stacking with a distance of 3.808(2) Å (Fig. S8). C–H···π interactions exist between H(1) and Cg(10) [C(40), C(41), C(42), C(43), C(44), C(45)] and H(42) and Cg(3) [C(1), C(2), C(3), C(4), C(5), C(6)] (Fig. S9). Weak N–O···π interactions are also present in the complex. The π···π, C–H···π and N–O···π interactions support the packing stability in the absence of strong conventional hydrogen bonds.

Fig. 10

Conclusion

Four dioxidomolybdenum(VI) complexes using two different ONO tridentate aroylhydrazones were synthesized, then spectroscopically and structurally characterized. All the complexes exhibit a distorted octahedral geometry whose sixth labile coordination site is occupied by a solvent molecule (water or DMF) or a heterocyclic base (4,4′-bipyridine). We were also able to synthesize mononuclear (**2**) as well as binuclear (**3**) complexes using the same reactants, but differing their molar ratios. Large Mo–X bond lengths (X = labile site) in the complexes can be used for application purposes and among the complexes synthesized, $[(MoO_2(L^1))_2(4,4'\text{-bipy})]\cdot 2H_2O$ (**3**) has the highest Mo–X bond length (2.439(2) Å). The different packing arrangements of the complex motif and supramolecular architectures formed by the influence of hydrogen bonding and weak non-covalent forces were also investigated.

Supporting Information

The tables and figures, including hydrogen bonding and non-bonding interactions, IR and UV-Vis spectra are included.

Acknowledgments

AAA and BJ acknowledge CSIR for the award of a Senior Research Fellowship. The ULK acknowledges UGC for the financial support. The authors are thankful to the Sophisticated Analytical Instrumentation Facility, Cochin University of Science and Technology, Kochi, India for elemental analyses and single crystal X-ray diffraction measurements.

Appendix A. Supplementary data

Crystallographic data for the structural analyses have been deposited with the Cambridge Crystallographic Data Center as CCDC 1506862, 1506864, 1506869 and 1506904 for the complexes $[MoO_2(L^1)(H_2O)]$ (**1**), $[MoO_2(L^1)(H_2O)]\cdot$(4,4′-bipy) (**2**), $[(MoO_2(L^1))_2$(4,4′-bipy)$]\cdot 2H_2O$ (**3**) and $[(MoO_2(L^2)(DMF)]$ (**4**) respectively. Copies of this information may be obtained free of charge *via* www.ccdc.cam.ac.uk/conts/retrieving.html or from the Director, CCDC, 12 Union Road, Cambridge, CB2 1EZ, UK (fax: +44-1223-336-033; e-mail: deposit@ccdc.cam.ac.uk).

References

[1] S.Y. Ebrahimipour, I. Sheikhshoaie, J. Simpson, H. Ebrahimnejad, M. Dusek, N. Kharazmi, V. Eigner, New J. Chem. 40 (2016) 2401-2412.

[2] J. Deng, Y. Gou, W. Chen, X. Fu, H. Deng, Bioorg. Med. Chem. 24 (2016) 2190-2198.

[3] X. Zhao, X. Chen, J. Li, J. Chen, G. Sheng, F. Niu, D. Qu, Y. Huo, H. Zhu, Z. You, Polyhedron 97 (2015) 268-272.

[4] M. Sutradhar, E.C.B.A. Alegria, K.T. Mahmudov, M.F.C.G. da Silva, A.J.L. Pombeiro, RSC Adv. 6 (2016) 8079-8088.

[5] I. Sheikhshoaie, S.Y. Ebrahimipour, M. Sheikhshoaie, H.A. Rudbari, M. Khaleghi, G. Bruno, Spectrochim. Acta 124A (2014) 548-555.

[6] R. Bikas, N. Noshiranzadeh, L. Sieroń, J.M. Barandiaran, T. Lis, J. Alanso, Inorg. Chem. Commun. 67 (2016) 85-89.

[7] M.A. Hussein, T.S. Guan, R.A. Haque, M.B.K. Ahamed, A.M.S.A. Majid, Inorg. Chim. Acta 421 (2014) 270-283.

[8] N. Mathew, M.R.P. Kurup, Spectrochim. Acta A78 (2011) 1424-1428.

[9] M.E. Judmaier, C.H. Sala, F. Belaj, M. Volpe, N.C. Mösch-Zanetti, New J. Chem. 37 (2013) 2139-2149.

[10] H. Sugimoto, M. Sato, L.J. Giles, K. Asano, T. Suzuki, M.L. Kirk, S. Itoh, Dalton Trans. 42 (2013) 15927-15930.

[11] K. Užarević, G. Pavlović, M. Cindrić, Polyhedron 52 (2013) 294-300.

[12] E.B. Seena, M.R.P. Kurup, Polyhedron 26 (2007) 3595-3601.

[13] M. Bagherzadeh, M.M. Haghdoost, A. Ghanbarpour, M. Amini, H.R. Khavasi, E. Payab, A. Ellern, L.K. Woo, Inorg. Chim. Acta 411 (2014) 61-66.

[14] G. Romanowski, J. Kira, Polyhedron 117 (2016) 352-358.

[15] N. García, R. Rubio-Presa, P. García-García, M.A. Fernández-Rodríguez, M.R. Pedrosa, F.J. Arnáiz, R. Sanz, Green Chem. 18 (2016) 2335-2340.

[16] S. Rakshit, D. Palit, S. K.S. Hazari, S. Rabi, T. G. Roy, F. Olbrich, D. Rehder, Polyhedron 117 (2016) 224-230.

[17] M.A. Hussein, T.S. Guan, R.A. Haque, M.B.K. Ahamed, A.M.S.A. Majid, Polyhedron 85 (2015) 93-103.

[18] D. Biswal, N.R. Pramanik, S. Chakrabarti, N. Chakraborty, K. Acharya, S.S. Mandal, S. Ghosh, M.G.B. Drew, T.K. Mondal, S. Biswas, New J. Chem. 39 (2015) 2778-2794.

[19] S. Pasayat, S.P. Dash, Saswati, P.K. Majhi, Y.P. Patil, M. Nethaji, H.R. Dash, S. Das, R. Dinda, Polyhedron 38 (2012) 198-204.

[20] R.J. Kunnath, M. Sithambaresan, A.A. Aravindakshan, A. Natarajan, M.R.P. Kurup, Polyhedron 113 (2016) 73-80.

[21] M. Đaković, D.V.-Viçosa, M.J. Calhorda, Z. Popović, Cryst. Eng. Comm. 13 (2011) 5863-5871.

[22] N.R. Pramanik, M. Chakraborty, D. Biswal, S.S. Mandal, S. Ghosh, S. Chakrabarti, W.S. Sheldrick, M.G.B. Drew, T.K. Mondal, D. Sarkar, Polyhedron 85 (2015) 196-207.

[23] N.K. Ngan, K.M. Lo, C.S.R. Wong, Polyhedron 33 (2012) 235-251.

[24] M.D. Ward, Chem. Soc. Rev. 24 (1995) 121-134.

[25] V. Vrdoljak, B. Prugovečki, D. Matković-Čalogović, T. Hrenar, R. Dreos, P. Siega, Cryst. Growth Des. 13 (2013) 3773-3784.

[26] B. Joseph, M. Sithambaresan, M.R.P. Kurup, Acta Cryst. E69 (2013) o1160-o1161.

[27] SMART and SAINT, Area Detector Software Package and SAX Area Detector Integration Program, Bruker Analytical X-ray, Madison, WI, USA, 1997.

[28] SADABS, Area Detector Absorption Correction Program; Bruker Analytical X-ray; Madison, WI, 1997.

[29] G.M. Sheldrick, Acta Cryst. C71 (2015) 3-8.

[30] L.J. Farrugia, J. Appl. Cryst. 45 (2012) 849-854.

[31] K. Brandenburg, Diamond Version 3.2g, Crystal Impact GbR, Bonn, Germany, 2010.

[32] W.J. Geary, Coord. Chem. Rev. 7 (1971) 81-122.

[33] M. Nandy, S. Shit, C. Rizzoli, G. Pilet, S. Mitra, Polyhedron 88 (2015) 63-72.

[34] (a) B.N.B. Raj, M.R.P. Kurup, E. Suresh, Spectrochim. Acta 71A (2008) 1253-1260.

(b) M. Kuriakose, M.R.P. Kurup, E. Suresh, Spectrochim. Acta 66A (2007) 353-358.

(c) B.N.B. Raj, M.R.P. Kurup, Spectrochim. Acta 66A (2007) 898-903.

(d) B.N.B. Raj, M.R.P. Kurup, E. Suresh, Struct. Chem. 17 (2006) 201-208.

[35] S.Y. Ebrahimipour, H. Khabazadeh, J. Castro, I. Sheikhshoaie, A. Crochet, K.M. Fromm, Inorg. Chim. Acta 427 (2015) 52-61.

[36] V. Stefov, V.M. Petrusevski, B. Soptrajanov, J. Mol. Struct. 293 (1993) 97-100.

[37] K. Jayakumar, M. Sithambaresan, A.A. Aravindakshan, M.R.P. Kurup, Polyhedron 75 (2014) 50-56.

[38] K. Nakamoto, Infrared and Raman Spectra of Inorganic and Coordination Compounds, 5th ed., John Wiley & Sons, NewYork, 1997, p.86.

[39] S. Sinha, M. Chakraborty, N.R. Pramanik, T.K. Raychaudhuri, T.K. Mondal, D. Sarkar, M.G.B. Drew, S. Ghosh, S.S. Mandal, Polyhedron 55 (2013) 192-200.

[40] J. Metz, O. Schneider, M. Hanack, Spectrochim. Acta. 38A (1982) 1265-1273.

[41] D. Cremer, J.A. Pople, J. Am. Chem. Soc. 97 (1975) 1354-1358.

[42] S.T. Rao, E. Westhof, M. Sundaralingam, Acta Cryst. A37 (1981) 421-425.

[43] N.K. Ngan, R.C.S. Wong, K.M. Lo, S.W. Ng, Acta Cryst. E67 (2011) m747.

[44] G.G. Evans, J.A. Boeyens, Acta Cryst. B45 (1989) 581-590.

[45] (a) R. Dinda, S. Ghosh, L.R. Falvello, M. Tomás, T.C.W. Mak, Polyhedron 25 (2006) 2375-2382.

(b) S. Alghool, C. Slebodnick, Polyhedron 67 (2014) 11-18.

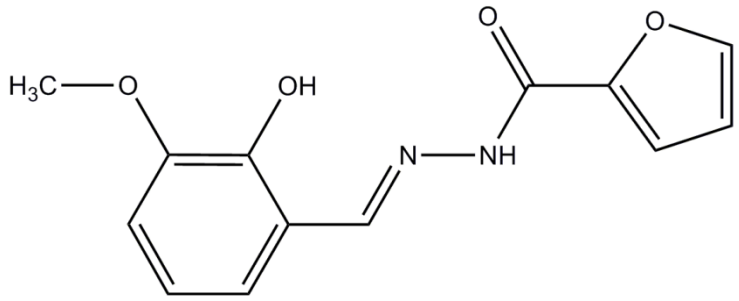

3-Methoxy-2-hydroxybenzaldehyde-2-furoic acid hydrazone (H_2L^1)

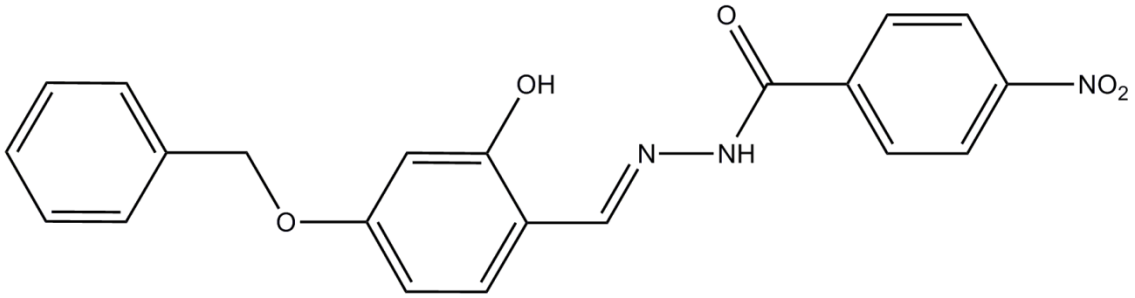

4-Benzyloxy-2-hydroxybenzaldehyde 4-nitrobenzoic hydrazone (H_2L^2)

Scheme 1. Structures of the tridentate ONO donor aroylhydrazones.

Table 1. Crystallographic data and structure refinement for **1**, **2**, **3** and **4**

Parameters	**1**	**2**	**3**	**4**
Empirical formula	$C_{13}H_{12}MoN_2O_7$	$C_{18}H_{16}MoN_3O_7$	$C_{36}H_{32}Mo_2N_6O_{14}$	$C_{24}H_{22}MoN_4O_8$
Formula weight	404.19	482.28	964.56	590.40
Crystal system	Monoclinic	Triclinic	Triclinic	Triclinic
Space group	$P2_1/c$	$P\bar{1}$	$P\bar{1}$	$P\bar{1}$
Cell parameters				
a (Å)	9.3396(7)	8.0905(4)	7.6833(3)	14.0681(12)
b (Å)	10.1066(7)	10.2535(5)	10.2972(4)	14.0982(12)
c (Å)	15.5078(12)	12.8847(7)	12.4364(5)	15.2049(12)
α (°)	90	76.608(3)	71.555(2)	95.301(3)
β (°)	97.872(2)	75.849(2)	79.260(2)	114.053(3)
γ (°)	90	69.484(2)	88.556(2)	111.047(3)

Volume V ($Å^3$)	1450.01(19)	958.08(9)	916.43(6)	2467.2(4)
Z	4	2	1	4
Calculated density (ρ) ($Mg\ m^{-3}$)	1.852	1.672	1.748	1.589
Absorption coefficient, μ (mm^{-1})	0.944	0.731	0.765	0.588
F(000)	808	486	486	1200
Crystal size (mm^3)	0.40 x 0.32 x 0.28	0.35 x 0.30 x 0.30	0.30 x 0.25 x 0.20	0.40 × 0.35 × 0.30
θ range for data collection	2.652 to 28.307°	2.73 to 25.05°	2.700 to 28.337°	1.80 to 27.00°
Limiting indices	$-12 \le h \le 10$ $-8 \le k \le 13$ $-20 \le l \le 20$	$-9 \le h \le 9$ $-12 \le k \le 12$ $-14 \le l \le 15$	$-9 \le h \le 10$ $-12 \le k \le 13$ $-16 \le l \le 16$	$-14 \le h \le 17$, $-18 \le k \le 12$, $-19 \le l \le 19$
Reflections collected/ Unique Reflections (R_{int})	10490 / 3614 [R(int) = 0.0360]	5779 / 3395 [R(int) = 0.0196]	7334 / 4571 [R(int) = 0.0224]	17880/10768 [R(int) = 0.0204]
Completeness to θ	25.242 (99.7%)	25.05 (99.3%)	25.242 (98.5%)	27.00 (98.0%)
Absorption correction	Semi-empirical from equivalents	Semi-empirical from equivalents	Semi-empirical from equivalents	Semi-empirical from equivalents
Maximum and minimum transmission	0.740 and 0.560	0.803 and 0.774	0.820 and 0.750	0.838 and 0.790
Data / restraints / parameters	3557 / 0 / 217	3370 / 3 / 272	4446 / 3 / 271	10548 / 0 / 672
Goodness-of-fit on F^2	1.012	0.946	1.042	1.031
Final R indices [$I > 2\sigma(I)$]	$R_1 = 0.0316$, $wR_2 = 0.0700$	$R_1 = 0.0238$, $wR_2 = 0.0641$	$R_1 = 0.0334$, $wR_2 = 0.0761$	$R_1 = 0.0377$, $wR_2 = 0.0919$
R indices (all data)	$R_1 = 0.0436$, $wR_2 = 0.0781$	$R_1 = 0.0270$, $wR_2 = 0.0695$	$R_1 = 0.0417$, $wR_2 = 0.0807$	$R_1 = 0.0573$, $wR_2 = 0.1059$
Largest difference peak and hole ($e\ Å^{-3}$)	0.572 and -1.056	0.433 and -0.432	0.438 and -0.408	1.063 and -0.649

$R_1 = \Sigma||F_o| - |F_c|| / \Sigma|F_o|$ $\quad$ $wR_2 = [\Sigma w(F_o^2-F_c^2)^2 / \Sigma w(F_o^2)^2]^{1/2}$

Table 2. Colors, partial elemental analyses and molar conductivity measurements of the dioxidomolybdenum(VI) complexes of ONO donor aroylhydrazones

Compounds	Color	Found (Calc.) %			Λ^*_M
		C	H	N	
$[MoO_2(L^1)(H_2O)]$ (**1**)	Orange	38.06 (38.63)	2.43 (2.99)	6.81 (6.93)	4
$[MoO_2(L^1)(H_2O)]\cdot$(4,4′-bipy) (**2**)	Orange	49.10 (49.30)	3.63 (3.60)	9.81 (10.00)	6
$[(MoO_2(L^1))_2$(4,4′-bipy)$]\cdot 2H_2O$ (**3**)	Dark red	45.10 (44.83)	3.63 (3.34)	8.81 (8.71)	6
$[MoO_2(L^2)(DMF)]$ (**4**)	Orange	48.98 (48.82)	3.93 (3.76)	9.87 (9.49)	11

* 10^{-3} M solutions in DMF

Table 3. Selected bond lengths (Å) and bond angles (°) of compounds **1**-**4**

Bond lengths (Å)							
$[MoO_2(L^1)(H_2O)]$ (**1**)		$[MoO_2(L^1)(H_2O)]\cdot$(4,4′-bipy) (**2**)		$[(MoO_2(L^1))_2$(4,4′-bipy)$]\cdot 2H_2O$ (**3**)		$[MoO_2(L^2)(DMF)]$ (**4**)	
Mo1–O2	1.9918(18)	Mo1–O2	1.9209(18)	Mo1–O2	1.9288(18)	Mo1–O2	1.923(2)
Mo1–N1	2.252(2)	Mo1–N1	2.242(2)	Mo1–N1	2.232(2)	Mo1–N1	2.217(2)
Mo1–O3	2.0018(18)	Mo1–O3	2.0157(17)	Mo1–O3	2.0088(18)	Mo1–O3	2.009(2)
Mo1–O5	1.682(2)	Mo1–O5	1.6880(18)	Mo1–O5	1.701(2)	Mo1–O6	1.705(2)
Mo1–O6	1.699(2)	Mo1–O6	1.6995(18)	Mo1–O6	1.6978(17)	Mo1–O7	1.689(2)
Mo1–O7	2.320(2)	Mo1–O1W	2.2425(18)	Mo1–N3	2.439(2)	Mo1–O8	2.341(2)
C8–N1	1.292(3)	C8–N1	1.291(3)	C8–N1	1.288(3)	C14–N1	1.289(4)
N1–N2	1.398(3)	N1–N2	1.391(3)	N1–N2	1.394(3)	N1–N2	1.391(3)
C9–N2	1.306(3)	C9–N2	1.298(3)	C9–N2	1.298(3)	C15–N2	1.292(4)
C9–O3	1.318(3)	C9–O3	1.306(3)	C9–O3	1.327(3)	C15–O3	1.316(3)

						Mo2–O10	1.923(2)
						Mo2–N5	2.218(2)
						Mo2–O11	2.007(2)
						Mo2–O14	1.682(2)
						Mo2–O15	1.701(2)
						Mo2–O16	2.351(2)
						C38–N5	1.292(4)
						N5–N6	1.392(3)
						C39–N6	1.294(4)
						C39–O11	1.313(3)
Bond angles (°)							
$[MoO_2(L^1)(H_2O)]$ (**1**)		$[MoO_2(L^1)(H_2O)]\cdot$(4,4′-bipy) (**2**)		$[(MoO_2(L^1))_2$(4,4′-bipy)$]\cdot 2H_2O$ (**3**)		$[MoO_2(L^2)(DMF)]$ (**4**)	
O5–Mo1–O7	169.53(11)	O5–Mo1–O1W	170.28(8)	O5–Mo1–N3	172.69(8)	O7–Mo1–O8	170.90(9)
O6–Mo1–N1	158.89(11)	O6–Mo1–N1	158.08(8)	O6–Mo1–N1	159.23(8)	O6–Mo1–N1	158.54(10)
O2–Mo1–O3	149.79(8)	O2–Mo1–O3	151.60(8)	O2–Mo1–O3	148.94(8)	O2–Mo1–O3	149.74(9)
O5–Mo1–O6	105.65(13)	O5–Mo1–O6	105.38(9)	O5–Mo1–O6	105.51(9)	O6–Mo1–O7	104.84(11)
O6–Mo1–O2	102.50(10)	O6–Mo1–O2	102.88(9)	O6–Mo1–O2	105.04(8)	O6–Mo1–O2	102.31(9)
O5–Mo1–O2	99.18(10)	O6–Mo1–O3	98.33(8)	O5–Mo1–O2	98.79(9)	O7–Mo1–O2	99.95(12)
O6–Mo1–O3	97.38(9)	O5–Mo1–O2	97.82(9)	O5–Mo1–O3	98.51(9)	O6–Mo1–O3	97.19(9)
O5–Mo1–O3	97.07(10)	O5–Mo1–N1	95.07(8)	O6–Mo1–O3	94.88(8)	O7–Mo1–O3	97.10(11)
O5–Mo1–N1	93.91(10)	O5–Mo1–O3	94.49(9)	O5–Mo1–N1	92.46(9)	O7–Mo1–N1	95.07(10)
O6–Mo1–O7	84.49(12)	O2–Mo1–O1W	83.89(9)	O2–Mo1–N1	81.88(8)	O6–Mo1–O8	83.13(9)
O2–Mo1–N1	81.83(8)	O6–Mo1–O1W	83.44(8)	O6–Mo1–N3	81.80(8)	O2–Mo1–O8	82.29(9)
O2–Mo1–O7	80.98(8)	O2–Mo1–N1	81.64(7)	O3–Mo1–N3	80.61(8)	O2–Mo1–N1	81.64(9)
O3–Mo1–O7	78.53(8)	O3–Mo1–O1W	79.98(8)	N1–Mo1–N3	80.36(7)	O3–Mo1–O8	77.29(8)
N1–Mo1–O7	75.72(9)	N1–Mo1–O1W	75.66(7)	O2–Mo1–N3	78.98(8)	N1–Mo1–O8	76.46(8)
O3–Mo1–N1	71.78(8)	O3–Mo1–N1	71.83(7)	O3–Mo1–N1	71.78(7)	O3–Mo1–N1	72.07(9)
						O14–Mo2–O16	170.79(10)
						O15–Mo2–N5	159.40(11)
						O10–Mo2–O11	149.27(9)
						O14–Mo2–O15	104.87(12)
						O15–Mo2–O10	102.52(10)
						O14–Mo2–O10	100.83(12)
						O15–Mo2–O11	97.47(10)
						O14–Mo2–O11	96.23(11)
						O14–Mo2–N5	94.12(10)

O15–Mo2–O16	83.52(10)
O10–Mo2–N5	81.23(9)
O10–Mo2–O16	80.67(10)
O11–Mo2–O16	78.65(9)
N5–Mo2–O16	77.07(8)
O11–Mo2–N5	72.16(8)

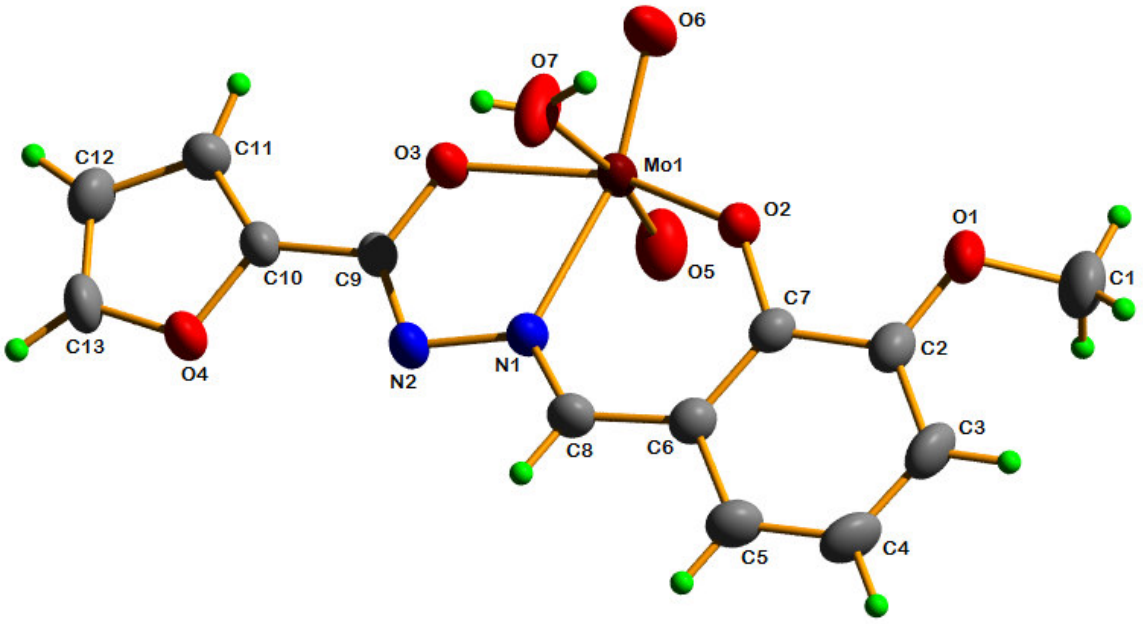

Fig. 1. Molecular structure of $[MoO_2(L^1)(H_2O)]$ (**1**), along with the atom numbering scheme.

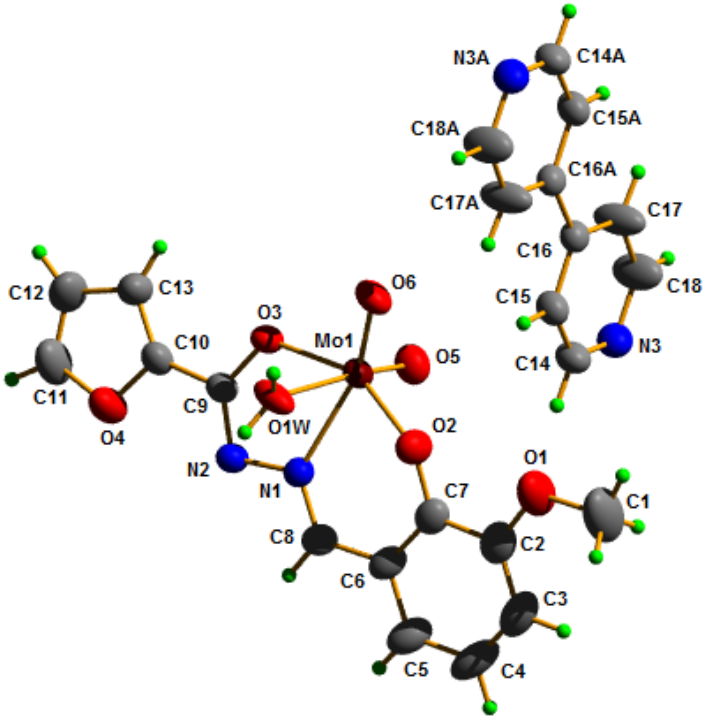

Fig. 2. Molecular structure of $[MoO_2(L^1)(H_2O)]\cdot$(4,4′-bipy) (**2**), along with the atom numbering scheme.

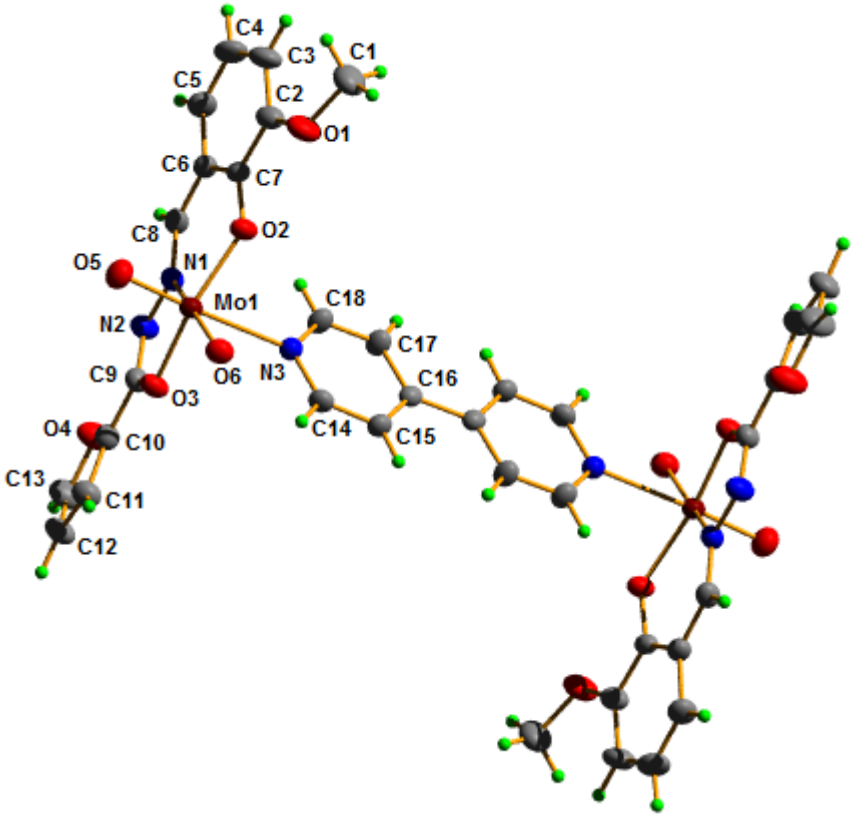

Fig. 3. Molecular structure of $[(MoO_2(L^1))_2(4,4'\text{-bipy})]\cdot 2H_2O$ (**3**), along with the atom numbering scheme. Two solvent water molecules are omitted for clarity.

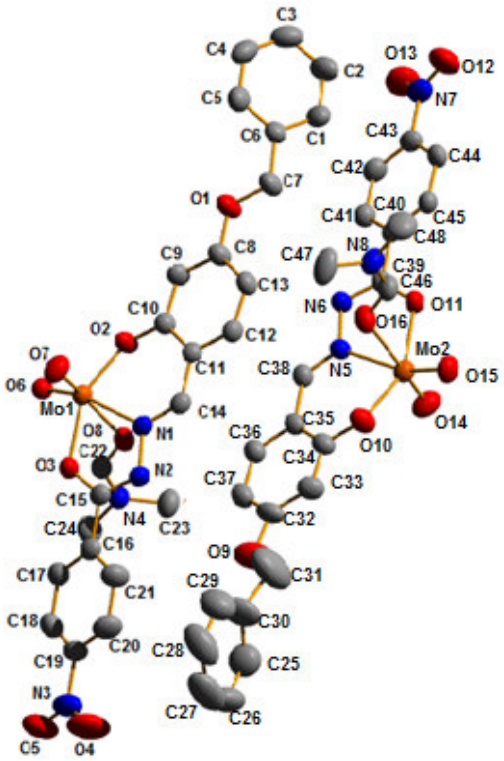

Fig. 4. Asymmetric unit of $[MoO_2(L^2)(DMF)]$ (**4**) (hydrogen atoms are omitted for clarity), along with the atom numbering scheme.

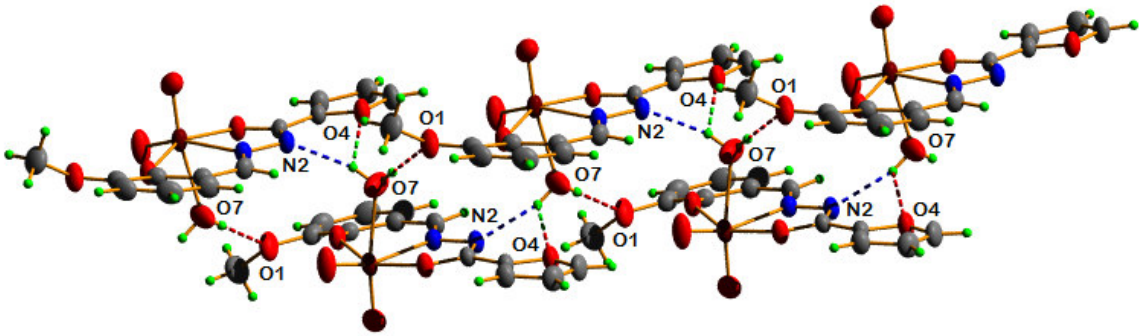

Fig. 5. Conventional hydrogen bonding interactions present in $[MoO_2(L^1)(H_2O)]$ (**1**).

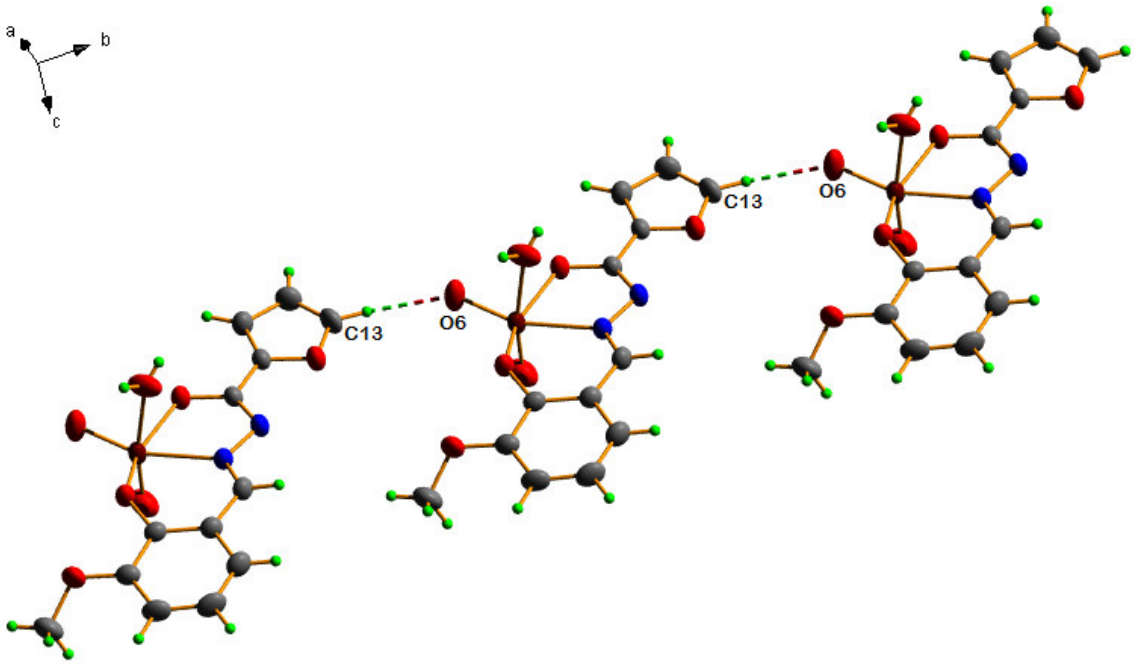

Fig. 6. C–H···O hydrogen bonding interactions in **1** connecting the molecules in a linear fashion propagating along the *b* direction.

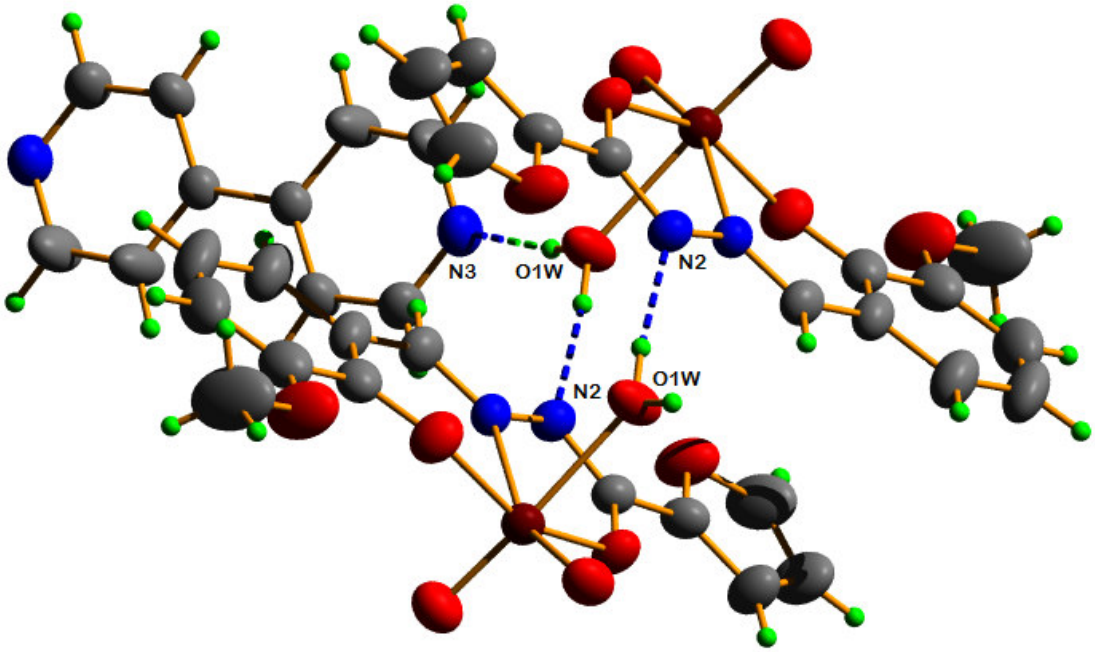

Fig. 7. Conventional hydrogen bonding interactions present in $[MoO_2(L^1)(H_2O)]\cdot(4,4'$-bipy) (**2**).

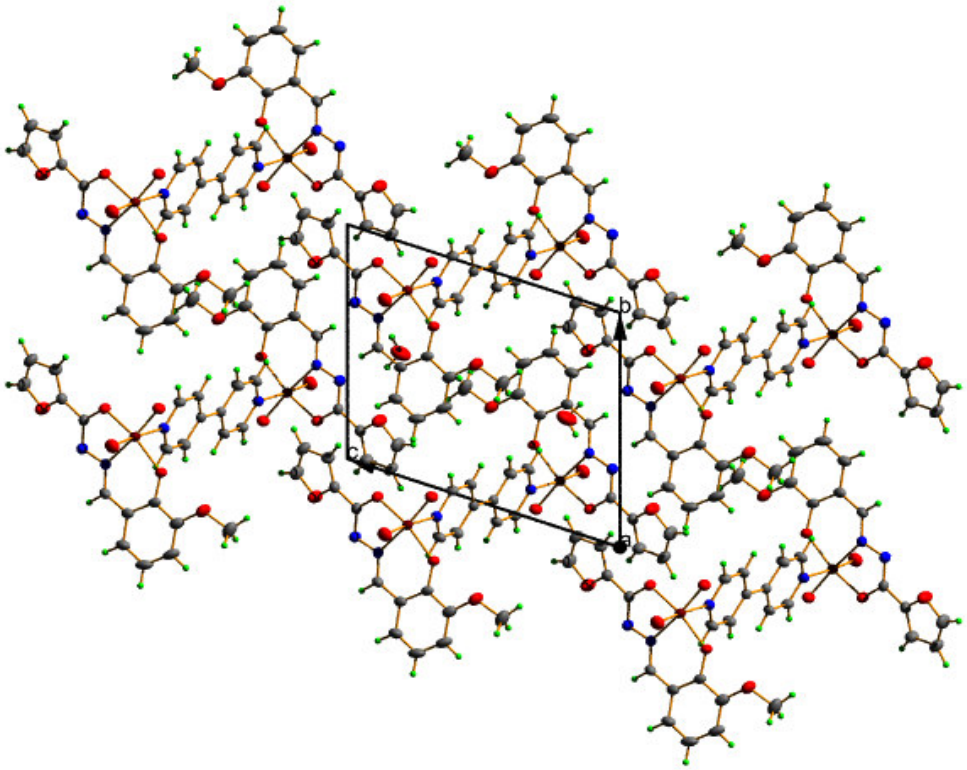

Fig. 8. The H-shaped complex motifs of $[(MoO_2(L^1))_2(4,4'\text{-bipy})]\cdot 2H_2O$ (**3**) packed in the crystal lattice when viewed along the crystallographic *a* axis.

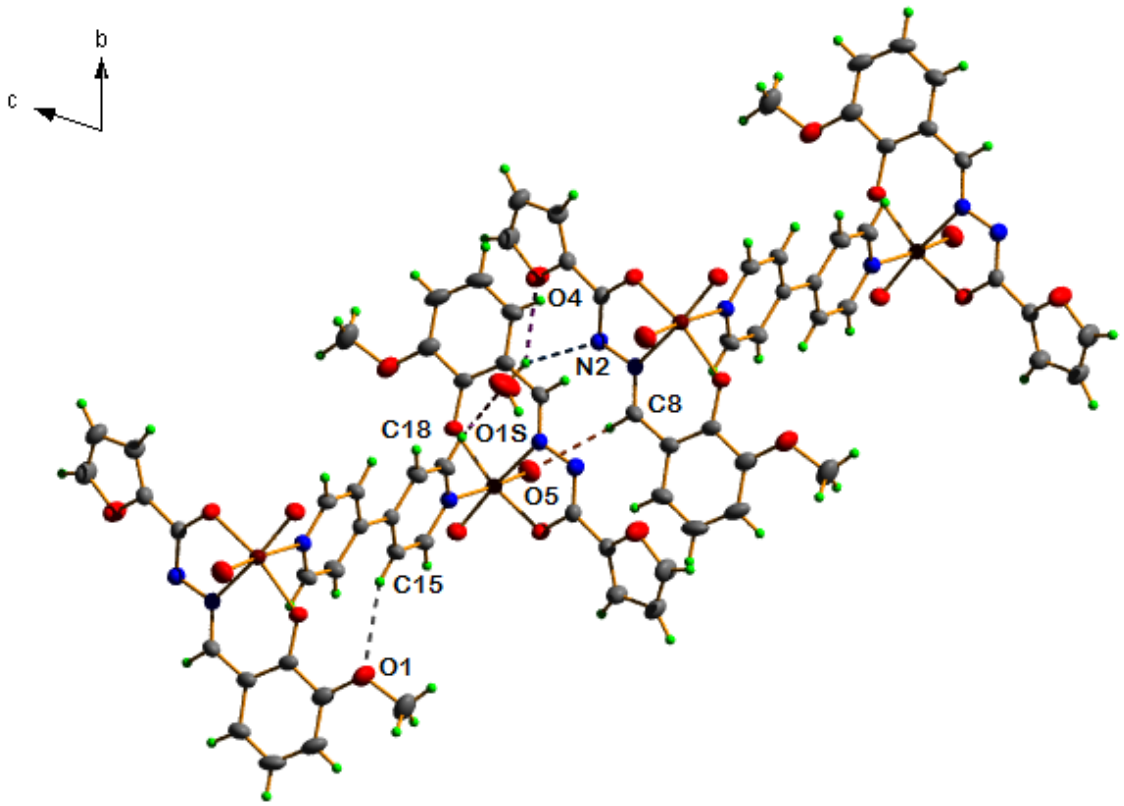

Fig. 9. The hydrogen bonding interactions in $[(MoO_2(L^1))_2(4,4'\text{-bipy})]\cdot 2H_2O$ (**3**) connecting the molecules when viewed along the crystallographic *a* axis.

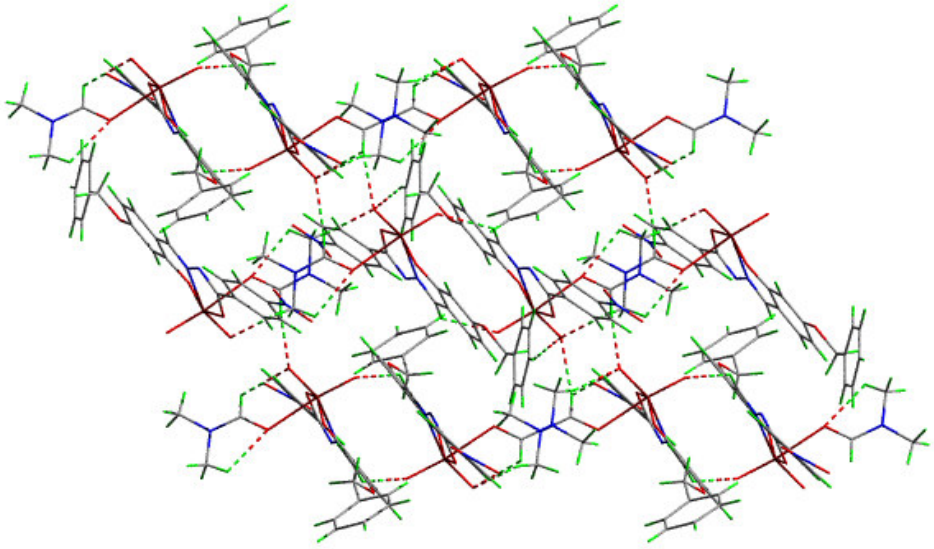

Fig. 10. Supramolecular chain mediated by non-conventional hydrogen bonding interactions in $[MoO_2(L^2)(DMF)]$ (**4**).

Graphical abstract

Three mononuclear complexes and one binuclear dioxidomolybdenum(VI) complex of two different tridentate aroylhydrazone ligands have been synthesized and physico-chemically characterized. Their crystal structures showed that all the complexes displayed a distorted octahedral geometry whose sixth labile coordination site is satisfied by a solvent molecule (water or DMF) or a heterocyclic base (4,4'-bipyridine). The bidentate ligand, 4,4′-bipyridine serve as a linker as well as an adduct in the complexes, which can be achieved by controlling its molar ratio in the synthesis reaction. The crystal packing of the complex motifs, formed by the influence of hydrogen bonding and weak non-covalent forces, were also investigated.